

UNIVERSITY OF TARTU\
Faculty of Science and Technology
Institute of Physics

Peter Oshioke Nelson-Dogo

OPTICAL PROPERTIES OF TIN OXIDE

Masters' Thesis (30 ECTS)
Curriculum Material Science and Technology

Supervisors:
Aarne Kasikov, PhD
Aile Tamm, PhD

AUGUST 2023

Table of content.

Table of content	2
Abstract	3
Abstract in Estonian	3
LIST OF ABBREVIATIONS AND ACRONYMS	5
Background of study	6
1.1 Introduction.....	6
1.2 Subject Matter.....	7
1.3 Aims and Objectives.....	9
1.4 Justification.....	9
Literature Review	10
Method and Materials	13
3.1 Introduction to Ellipsometry.....	13
3.2 Optical Index representation.....	14
3.3 nk values / files.....	14
3.4 Dispersion law.....	15
3.5 Methodology.....	16
3.6 SnO ₂ Films.....	17
Results and conclusion	18
4.1. Energy(eV) Dependence.....	18
4.2 Temperature(oC) Dependence:.....	26
4.3. Conclusion.....	32
Reference	33

Abstract

This study explores the optical properties of thin films composed of Tin oxide (SnO_2) over a temperature range spanning from 100 °C to 600 °C. The films were deposited using ALD which has proven to be a reliable deposition method. The investigation encompasses the utilization of three distinct theoretical frameworks, namely the Tauc-Lorentz law, Cauchy Law and Cauchy-Lorentz law, to comprehensively characterize the optical behavior of the thin films. The spectral dependence of the refractive index (n) and extinction or absorption coefficient (k) is scrutinized across the temperature and energy spectrum, shedding light on the intricate interplay between material structure and thermal effects.

Using an Ellipsometer and its accompanying software, I was able to make iterations in which the final results were considered by features such as $R^2 > 0.97$ and also the absence of negative absorption.

In conclusion, this investigation presents a thorough analysis of the optical properties of tin oxide films over a temperature range of 100 °C to 600 °C. The amalgamation of the Tauc-Lorentz, Cauchy, and Cauchy-Lorentz laws provides a comprehensive framework for understanding the intricate interplay between material structure and temperature-dependent optical behavior. The findings contribute to the broader knowledge of thin film optics and offer valuable information for the development of temperature-sensitive optoelectronics technologies.

Abstract in Estonian

Töös uuritakse temperatuuride vahemikus 100 kuni 600 °C valmistatud tinaoksiidi (SnO₂) kihtide optilisi omadusi. Kiled olid valmistatud kasutades ALD (aatomkihtsadestamine), mis on end näidanud usaldusväärse kasvatusmeetodina. Uurimisel kasutati kilede optiliseks iseloomustamiseks 3 erinevat teoreetilist baasi – Tauc-Lorentzi, Cauchy ja Cauchy-Lorentzi dispersioonmudeleid. Määrati murdumisnäitaja (n) ja neeldumisnäitaja (neeldumiskoeffitsiendi) (k) temperatuuri- ja energia-spektraalsõltuvused, mis võimaldab heita pilgu materjali struktuuri ja termiliste efektide vahelistele seostele.

Kasutades ellipsomeetrit ja sellega kaasas olevat tarkvara, suutsin ma iteratsioonmeetodil jõuda tulemusteni, mille korral $R^2 > 0,97$ ja tulemustes puudub negatiivne neeldumine.

Kokku võttes – töö esitab tinaoksiidi optiliste omaduste analüüsi temperatuuride vahemikus 100 kuni 600 °C. Tauc-Lorentzi, Cauchy ja Cauchy-Lorentzi dispersioonseoste ühendamise annab põhja materjali struktuuri ja temperatuurist sõltuvate omaduste vastastikuse seose uurimiseks. Tulemused annavad panuse õhukeste kilede optika laiemasse tausta ja väärtuslikku informatsiooni temperatuuritundlike optoelektroniliste tehnoloogiate arengule.

LIST OF ABBREVIATIONS AND ACRONYMS

ALD - Atomic Layer Deposition
CL - Cauchy-Lorentz
CVD - Chemical Vapour Deposition
MBE- Molecular Beam Epitaxy
MOCVD - Metalorganic Chemical Vapor Deposition
PVD - Physical Vapor Deposition
 R^2 = Correlation Coefficient
TCO - Transparent Conducting Oxide
TL - Tauc-Lorentz
UV - Ultraviolet

Chapter 1

Background of study

1.1 Introduction

The field of science and technology has experienced a great turn since the discovery of the materials called thin films. There is rapid progress in integrating thin films into our everyday devices; this is because their properties such as electrical, optical, mechanical, chemical etc play crucial roles depending on the reason for their application. These unique materials are formed through a combination of chemical, physical and mechanical processes.

A thin film is a layer or layers of materials ranging from nanometers to micrometers in size and thickness. Thin films make use of the principle of evaporation and condensation. The resulting vapor is deposited on the surface of a material called the substrates which then solidifies to form a film. This process can be repeated at intervals until the desired thickness is achieved.

Advances in technology require the use of thin films. They possess convenient electrical and optical properties that are suitable for hard coatings, electronics etc. The properties of thin films are strongly dependent on the method of film growth, substrate and material. The production of thin films is widely distributed into Physical Vapour Deposition and Chemical Vapour Deposition.

These films, when fully harnessed by scientists, impact various areas of life positively: be it the military, government, nuclear science or technology as a whole etc.

Tin oxide (SnO_2) is a tetragonal n-type semiconductor with a wide energy band gap of about 3.6 eV, this semiconductor is suitable for vast application due to its low electrical resistivity and high optical transparency. This colorless, amphoteric solid is found in the earth crust and its ore is called Cassiterite. Because of its affordability, tin oxide is a perfect candidate for various applications such as gas sensors, conductive coatings, electrodes etc. Thin film production is an important aspect of nano-technology, this research project entails the production of tin oxide films, and a clear study of its optical properties.

1.2 Subject Matter

1.2.1 Physical Vapour deposition (PVD)

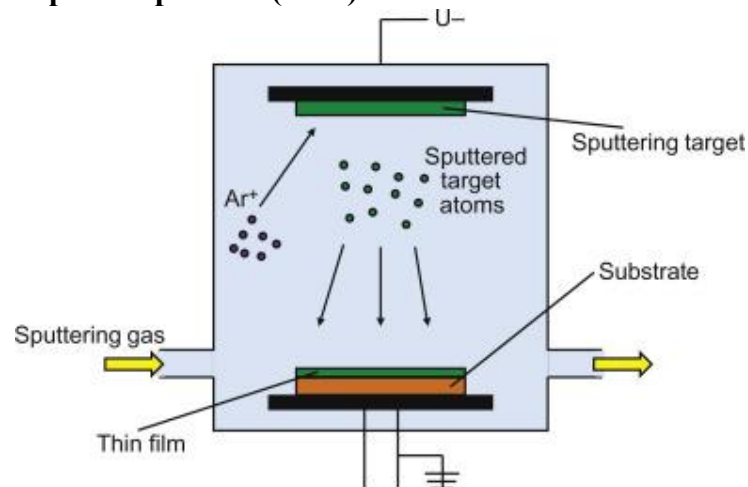


Fig 1: Diagrammatic representation of direct sputtering(a part of PVD) [1]^{int}

Physical method of deposition, otherwise known as physical vapor deposition, is a method of film growth that involves the transportation of vapor from its source material (Sputtering target in the figure 1 above) to the surface of the substrate, which then solidifies and forms a film. The source material is placed inside a chamber and during the process, the pressure is reduced. Pressure is reduced to give the vapor a possibility to reach the object. One major importance of using PVD is achieving high purity coatings, and offers the opportunity of tailoring the film properties. Since the vapor travels through a medium, a large range of substrates can be used. The most used form of PVD is vacuum evaporation which uses a heating device to evaporate the material onto the surface of the substrate.

1.2.2 Chemical Vapour deposition (CVD)

Chemical Vapour deposition is a method used in producing quality solid thin films. This process involves the reaction of a volatile precursor (halides, hydrides, metal compounds, and metal alkyls), to be deposited to produce nonvolatile solid thin films on substrates. The CVD technique supports the growth of pure thin films with uniformity in thickness and controlled porosity. CVD has one definite edge over other procedures because of its multidirectional deposition of thin films. Therefore, the shape of the substrate does not really matter. Some of the key advantages of using CVD include:

1. **Film Conformality:** CVD enables the deposition of thin films with excellent conformality, meaning the film can uniformly coat complex and 3-D structures. This capability makes CVD sometimes suitable for coating materials with high aspect ratios, such as nanopores, trenches, and patterned substrates[1].
2. **Precise Thickness Control:** CVD allows for precise control over film thickness. By controlling deposition parameters such as precursor flow rate, reaction time, and substrate temperature, the film thickness can be accurately controlled at the atomic or molecular level. This level of control is crucial for applications that require films of specific thicknesses for optimal performance.

3. Large -Scale Production: CVD is well suited for large scale production due to its ability to deposit thin films over a wide area. It can be integrated into batch processing systems or continuous roll-out setups, enabling high-throughput manufacturing of thin film coatings on large substrates.
4. Wide Range of Material: CVD can deposit films from a wide range of materials, including metals, semiconductors, oxides, nitrides, and carbon-based materials. This versatility allows for the deposition of films with diverse properties, such as electrical conductivity, optical transparency, hardness, and corrosion resistance.
5. Tailored Film Properties: CVD offers flexibility in tailoring film properties by adjusting deposition parameters and precursor chemistry. By selecting appropriate precursor and deposition conditions, it is possible to control the film's composition, crystallinity, microstructure, and surface morphology, thereby achieving specific material properties to meet application requirements.
6. Uniformity and Purity: CVD can produce thin films with high uniformity across the substrate surface, ensuring consistent performance and quality.

Due to these advantages, CVD finds applications in numerous fields, including semiconductor manufacturing, optoelectronics, photovoltaics, catalyst synthesis, corrosion protection, wear-resistant coatings and biomedical devices.

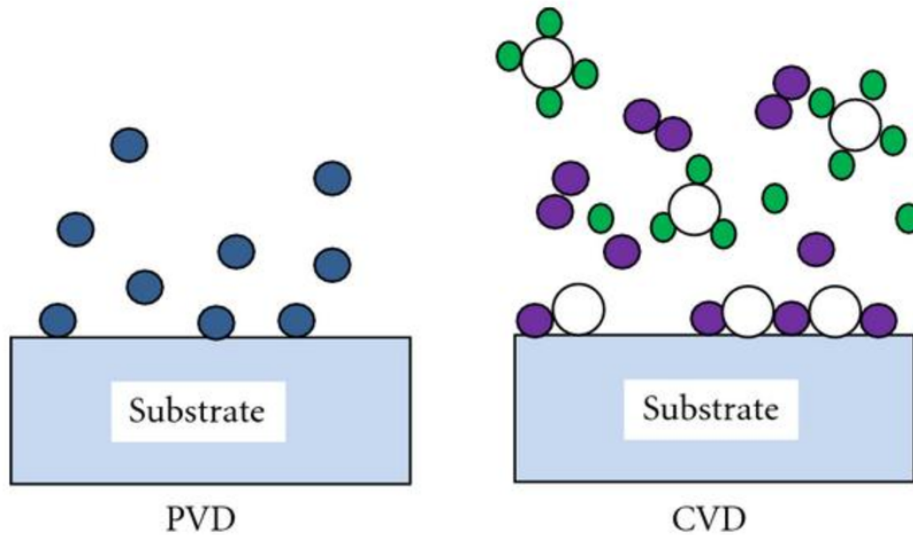


Fig 2: Difference between CVD and PVD|[2]^{na}

One very obvious difference between PVD and CVD is that the precursors of the physical method are the same as the resulting film. There is no chemical change.

1.2.3 Atomic Layer Deposition (ALD)

ALD is a method of thin film production that belongs to the broader class of CLD. This process is used to achieve the desired thickness of thin films. It is a combination of a physical method; MBE and CVD[3].

Atomic Layer Deposition (ALD). The working principles of ALD can be summarized as follows;

1. Self-limiting surface reactions: ALD relies on the use of self-limiting surface reactions between two or more precursor molecules and the substrate surface. During each ALD cycle, a single monolayer of material is deposited on the surface of the substrate, ensuring precise control over the thickness of the film[4].
2. Sequential alternating exposure: The deposition process involves alternating exposure of the substrate to two or more precursor molecules, typically in gaseous form, one at a time. Each precursor is introduced into the reactor chamber, where it reacts with the surface to form a chemisorbed layer.
3. Purging step: After each precursor exposure, the chamber is purged with an inert gas to remove any unreacted precursor molecules and reaction byproducts. These steps help ensure that the surface is prepared for the next precursor exposure.
4. Repeat cycle: the process is then repeated for as many cycles as necessary to achieve thickness. Number of cycles required depends on film thickness and the reactivity of the precursor molecules.
5. Temperature and pressure control: ALD is typically carried out at low pressure (10^{-2} to 10 Torr) and for some deposition at near atmospheric pressure (1 to 10^3 Torr). Temperatures used depend on the chamber, precursors and the substrate.

By following these principles, ALD can deposit uniform, conformal thin films with precise thickness control and excellent reproducibility. ALD has found widespread use in a variety of applications including semiconductor device fabrication, surface coatings and energy storage.

1.3 Aims and Objectives

- To grow high end quality thin films of Tin Oxide (SnO_2) using Atomic layer deposition.
- To study the optical properties of the produced film.
- Study areas in which the produced films can be applied to.

1.4 Justification

The world is growing rapidly in areas such as sensors, electrical devices and photonics. We continuously need materials that will give us new possibilities. This is possible with research on available thin-films materials as well as new ones. Thin films are now integral parts in electronics, solar panels and even household materials.

This research project explores the optical properties of Tin oxide thin-films made from ALD and Our task is to find the particular parameters of the obtained films using various models for optical analysis .

Chapter 2

Literature Review

There is an increasing study on the synthesis of thin films of tin oxide and their properties.

For instance, detecting H₂S is of great importance in commercial gas and oil exploration, auto ventilation units and the medical field. This is primarily because of its high toxicity. So back in 2002, *Arijit Chowdhuri, Paramanand Sharma, Vinay Gupta, K. Sreenivas and K.V. Rao et al.* studied the H₂S gas sensing mechanism of SnO₂ films with ultrathin CuO dotted islands. Changes induced on the surface due to variations in sensitivities for three different sensors; SnO₂, SnO₂-CuO and SnO₂ with CuO islands were considered[5].

By the year 2010, *Zhen Zhu, Jin Ma, Lingyi Kong, Caina Luan, Qiaoqun Yu et al* studied the optical and electrical properties of SnO₂ heteroepitaxy thin films on m-plane sapphire by MOCVD. X-ray diffraction showed the films' rutile structure and the film orientation were dependent on growth temperature. In the visible region, the samples showed high transparency of up to 80%[6].

In 2003, *Jonas Sundqvist, Aivar Tarre, Arnold Rosental et al.* deposited epitaxial and polycrystalline SnO₂ films from the SnI₄/O₂ precursor combination using atomic layer deposition. These were deposited on α -Al₂O₃(012) and SiO₂/Si(100) substrates at a temperature range between 400-750 °C. In general the growth rate was high, changing from 0.10 nm cycle⁻¹ at 500 °C to 0.12 nm cycle⁻¹ at 750 °C for the α -Al₂O₃(012) substrate, and from 0.04 nm cycle⁻¹ at 500 °C to 0.12 nm cycle⁻¹ at 750 °C for the SiO₂/Si(100) substrates. The growth rate on SiO₂/Si(100) was faster except at the lowest temperature of 400°C. The study was able to prove the possibility of growing Iodine free and phase-pure SnO₂ from SnI₄ and O₂ precursors using an ALD process[7].

In 2012, *M. Alaf, D. Gultekin and H. Akbulut et al.* made Sn/SnO₂ thin-films using thermal evaporation(a type of PVD) and plasma oxidation as anode for Li-ion batteries. The reason for this choice was because of the need to develop batteries that are more durable, nontoxic, inexpensive and with higher energy densities. SnO₂ has high theoretical capacity and good cycling stability. Using stainless steel substrates, pure metallic tin was thermally evaporated in the presence of argon and oxygen at a pressure of 1Pa. After the thermal evaporation, the tin samples were plasma oxidized using 3 different time processes; 30, 45 and 60 mins. The ratios of Sn:SnO₂ obtained were 82:18, 73:26 and 62:32. They were used as electrodes for Li-ion cells and their discharge capacities were seen to increase with increasing SnO₂ in the composite¹[8].

Using RF sputtering deposition in 2015, *A. Alhuthali et al.* studied the effect of different annealing temperatures (473 K, 673 K and 823 K) on the topological morphology and optical properties of SnO₂ thin films^[4]. This method is well known for its ability to produce homogenous and high quality thin films of various materials, especially TCO. It makes use of economical, efficient evaporants which can be modeled to industrial scale

for semiconductor production^[5]. As annealing temperature increased, the Urbach energies^[15] of the thin films reduced. Other characteristics which showed the quality of these thin films were the direct optical band gap (E_g^d) and the dispersion curves of the refractive index. E_g^d decreased as well with increasing annealing temperature and dispersion curves were found to obey the single oscillator model^[9].

The optical properties of SnO₂ continue to be an active area of research with promising future studies and applications. Here are some potential directions and applications for the future exploration of tin oxide's optical properties:

1. Optoelectronic Devices: Tin oxide has shown potential as a TCO material for optoelectronic devices, such as solar cells, light-emitting diodes (LEDs), displays. Future studies can focus on enhancing the electrical and optical properties of tin oxide, improving their transparency, conductivity, and light extraction efficiency for efficient and high-performance optoelectronic devices^[3].
2. Plasmonic and Metamaterials: Plasmonic effects and metamaterials can be achieved by integrating tin oxide's optical properties to design and fabricate plasmonic devices, such as surface-enhanced Raman spectroscopy (SERS) substrates, nanophotonic circuits, and active metasurfaces, enabling advanced light manipulation and control at the nanoscale^[4].
3. Photovoltaic and Energy Harvesting: Tin oxide can be employed as a material for transparent electrodes in solar cells and other energy harvesting devices. Future research can focus on improving the conductivity, light trapping, and charge extraction properties of tin oxide films to enhance the efficiency of the photovoltaic devices. Additionally, the development of tin oxide-based photocatalysts for solar-driven water splitting and other energy conversion applications is an area of interest^[10].
4. Gas Sensing and Environmental Monitoring: Tin oxide exhibits excellent gas sensing properties, making it a valuable material for gas sensors and environmental monitoring. Future studies can explore the optimization of tin oxide's optical properties for enhanced gas sensing technologies, such as optical fibers and micro/nanofabrication techniques, which can open up new avenues for highly sensitive and selective gas sensing devices^[6].
5. Optical Filters and Coatings: Tin oxide's tunable optical properties, including its refractive index and transmission range, make it suitable for optical filters, antireflection coatings and wavelength-selective coatings^[11].
6. Thin Film Optics and Nanophotonics: Tin oxide's thin films can be engineered to exhibit desired optical properties such as high transmittance, low reflectance, tailored dispersion characteristics. Future research can focus on developing advanced thin film optics and nanophotonic devices based on tin oxide, including waveguides, photonic crystals, and integrated photonics platforms^[10].

It is important to note that these are speculative areas and potential future directions for the study and application of tin oxide's optical properties. Continued research and technological advancements in material synthesis, characterisation techniques, and device fabrication will likely uncover new opportunities and applications for tin oxide in the field of optics and photonics.

Chapter 3

Method and Materials

3.1 Introduction to Ellipsometry.

Ellipsometry is an optical measurement technique that is commonly used to study the properties of thin films and surfaces. The technique is based on the principle that the polarization state of light is changed when it interacts with a material (only for oblique incidence), and that these changes can be used to obtain information about the properties of the material.

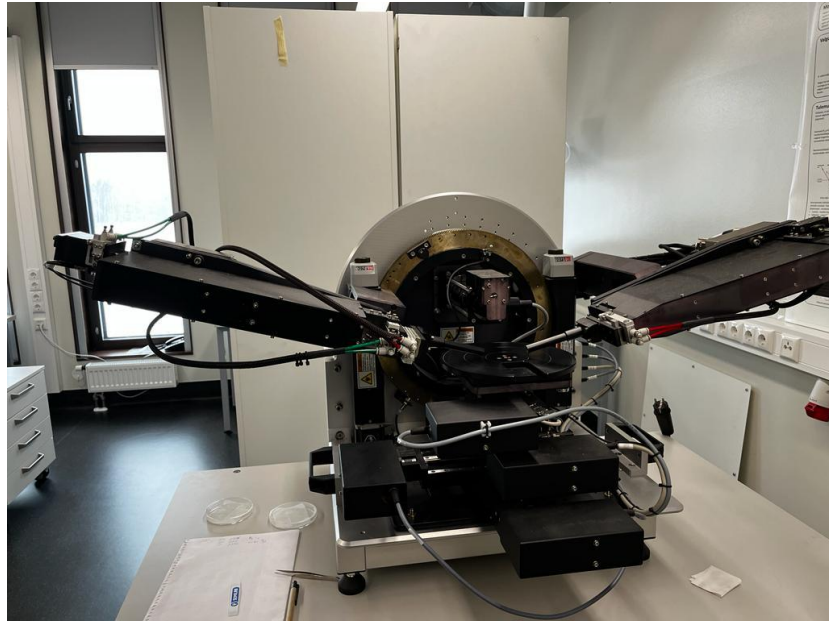


Fig 3 An Ellipsometer (At Physicum, University of Tartu, 2023)

One of the softwares used for ellipsometric and reflectometric analysis simulations is the WinElli II. We extracted sample parameters as accurately as possible and made a large range of optical simulations using this.

To start a simulation or make a regression, you are expected to define the structure of the sample. Different layers can make up the sample and they are defined according to a table. Available in this table include the following;

- Number of layers
- Description of the layer
- Thickness of the layer
- Optical index representation etc(WinElli User's manual for Ellipsometer)

3.2 Optical Index representation.

This refers to a way of representing the optical properties of a material in terms of its refractive index. Optical index representation is useful because it provides a convenient

way to compare the optical properties of different materials over a range of wavelengths. The different options available in the WinElli software are: nk file, mixed nk files, dispersion law, nk file and dispersion law, alloy, diffusion layer.

3.3 nk values / files

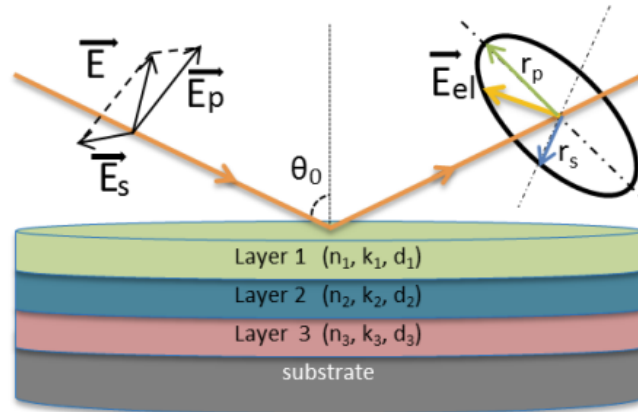


Fig 3.1 Multilayer showing the polarization of light

(A ray of linearly imposed light E incident on a film and the associated characteristics of each layer; n, k and d of the material reflecting an elliptically polarized wave)

In ellipsometry, the refractive index (n) and extinction coefficient (k) of a material are commonly represented as a complex quantity known as the complex refractive index $N = n - ik$. This complex quantity is obtained by analyzing the changes in the polarization of light that is reflected or transmitted by the sample. The changes in polarization are related to the optical properties of the sample, and can be used to extract information such as thickness, refractive index and other properties.

The values obtained are typically represented as a function of the wavelength of the light or energy used in measurement. This representation is often referred to as an “nk file”.

An ellipsometric measurement allows the determination of the phase difference, Δ , between reflected p- and s- polarizations of electric field of light and, $\tan \Psi$ which represents the ratio of their amplitudes. Ψ represents the angle which is determined from the amplitude ratio between reflected p- and s- polarized light.

$$\tan \Psi = |r_p| / |r_s| ,$$

$$\Delta = \delta r_p - \delta r_s$$

where, δr_p and δr_s are the phase changes at reflection and, r_p and r_s are originally defined by the ratios of reflected electric field to incident electric field for p and s components.

3.4 Dispersion law.

A mathematical model that allows us to simulate the optical indices (n&k) and their variations according to wavelength. Six types of dispersion laws can be defined from the WinElli II manual:

- Standard dielectric function
- Classical oscillator assembly
- Standard critical points
- Forouhi interband model
- Model dielectric function
- Tauc-Lorentz model

3.4.1 Cauchy law on n and k:

n and k are calculated with the expressions:

$$n = A + B / \lambda^2 + C / \lambda^4$$
$$k = D / \lambda + E / \lambda^3 + F / \lambda^5$$

A, B, C, E and F are treated as fitting parameters or coefficients that depend on the material.

The Cauchy model is a simple and widely used model for describing the refractive index of materials, particularly transparent materials such as glasses and polymers. However, it may not be accurate for materials with complex optical properties, where more complex models may be needed to describe the refractive index as a function of wavelength[9]

3.4.2 Lorentz Function

$$\epsilon_r = \frac{A * \lambda^2 * \left(\lambda^2 - \left(\frac{Kzero}{E_0} \right)^2 \right)}{\left(\lambda^2 - \left(\frac{Kzero}{E_0} \right)^2 \right)^2 + gamma^2 * \lambda^2}$$
$$\epsilon_i = \frac{A * \lambda^3 * gamma}{\left(\lambda^2 - \left(\frac{Kzero}{E_0} \right)^2 \right)^2 + gamma^2 * \lambda^2}$$

ϵ_i and ϵ_r are the dielectric constants of the material, A is the intensity, E_0 is the energy of the central wavelength, gamma is the width of the peak derived from the broadening parameter of the critical point and $Kzero = 1.239852066$ only if E_0 is presented in eV.

3.4.3 Cauchy-Lorentz model

This is a mathematical model used to describe the refractive index of a material as a function of the wavelength of light. It is a combination of the polynomial expression of the Cauchy model and the oscillatory expression of the Lorentz model.

k is got from the Lorentz function while that for Cauchy = 0
 $n_{\text{Cauchy}} + \text{Lorentz function}$.

3.4.4. Tauc-Lorentz model

The Tauc-Lorentz model is a combination of the Tauc and Lorentz models[12]. It is a mathematical formula for the frequency dependence of the complex-valued relative permittivity, sometimes referred to as dielectric functions. The Tauc-Lorentz model curve is typically plotted as the absorption coefficient (α) versus the photon energy.

$$\varepsilon_{i,L}(E) = \frac{A_L \cdot E_0 \cdot C \cdot E}{(E^2 - E_0^2)^2 + C^2 \cdot E^2}$$

Where:

- A_L is the strength of the peak
- C is the broadening term of the peak
- E_0 is the peak central energy

3.5 Methodology

1. Sample preparation:
 - Clean the sample surface thoroughly to remove contaminants.
 - Ensure the sample is stable and properly mounted in the ellipsometer's sample holder
2. Instrument Setup:
 - Turn on the ellipsometric spectrometer and allow it to warm up if needed.
 - Align the optical components, such as light sources and polarizers, according to the instrument's manual.
3. Basic Ellipsometric Measurement:
 - Choose an appropriate wavelength or eV range for your measurement. For my research, I used 1.2829 - 5.5000 eV
 - Set the initial measurement parameters (angle of incidence = 75°)
 - Perform a basic ellipsometric measurement by illuminating the sample with polarized light and measuring the change in polarization
4. Collecting Raw Data:
 - Measure the ellipsometric angles Ψ (Psi) and Δ (Delta) for each wavelength or measurement point.
 - Record the raw data (Ψ and Δ values) for further analysis.

5. Modeling:
 - I used the Winelli software to model the ellipsometric data.
6. Model Fitting:
 - Imputed initial estimates for film thickness, refractive index, and other parameters.
 - Software compares the modeled ellipsometric angles with the measured data and iteratively adjusts the parameters to minimize differences.
7. Extracting Optical properties:
 - Once fitting is successful, WinElli provides the best fit parameters including refractive index(n) and extinction coefficient(k) for each layer.
 - Other film properties like thickness and roughness can be extracted as well.
8. Data Analysis and Interpretation:
 - I analyzed the obtained optical properties to understand the behavior of the thin films

3.6 SnO₂ Films

Are well known n-type semiconductors with an indirect wide band gap of 3.6-3.8 eV[13]. The films for this research were deposited using ALD in 2021. SnI₄ and O₃ with a density of 240g/m³ were used as precursors. Process sequence was 5/2/5/5 s SnI₄/N₂ purge/O₃/N₂ purge. The samples sizes were 10*10 mm Si (natural oxide or HF-treated).

Chapter 4

Results and conclusion

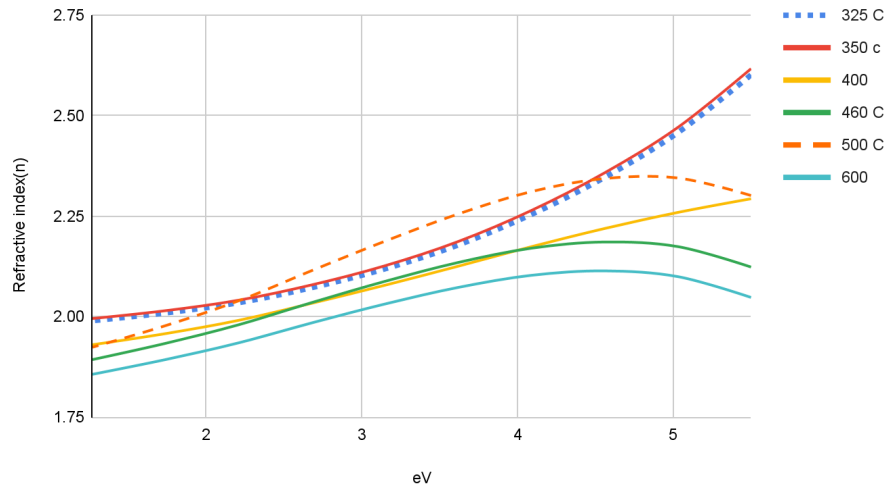
Three laws were used for the characterisation of SnO₂; Tauc-Lorentz, Cauchy, and Cauchy-Lorentz. The films deposited at various temperatures showed similar characteristic curves to one another.

4.1. Energy(eV) Dependence

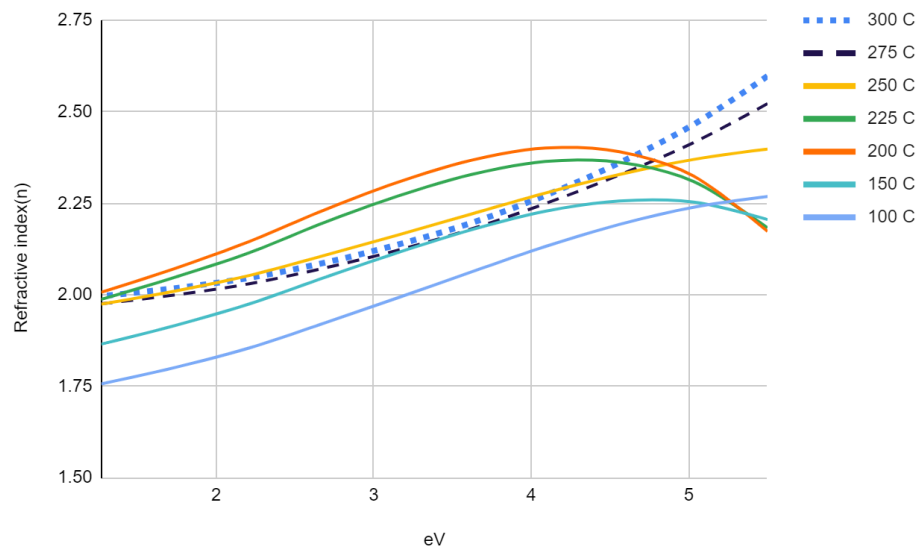
In many cases, the energy (or wavelength) dependence of optical properties is of high importance. This is particularly true in the context of light-matter interactions, where the energy of photons determines the nature of electronic transitions, absorption bands, and other optical phenomena. The energy dependence of optical properties dictates how materials interact with light of different wavelengths, affecting behaviors like colour perception, dispersion, and spectral filtering. For instance in spectroscopy the interaction of light with matter provides valuable information about the material's composition and properties, and in colour perception and display technologies used for producing LEDs, the energy dependence of light is critical for producing accurate and vibrant colors.

4.1.1 Refractive Index(n) vs Energy(eV)

Cauchy Law

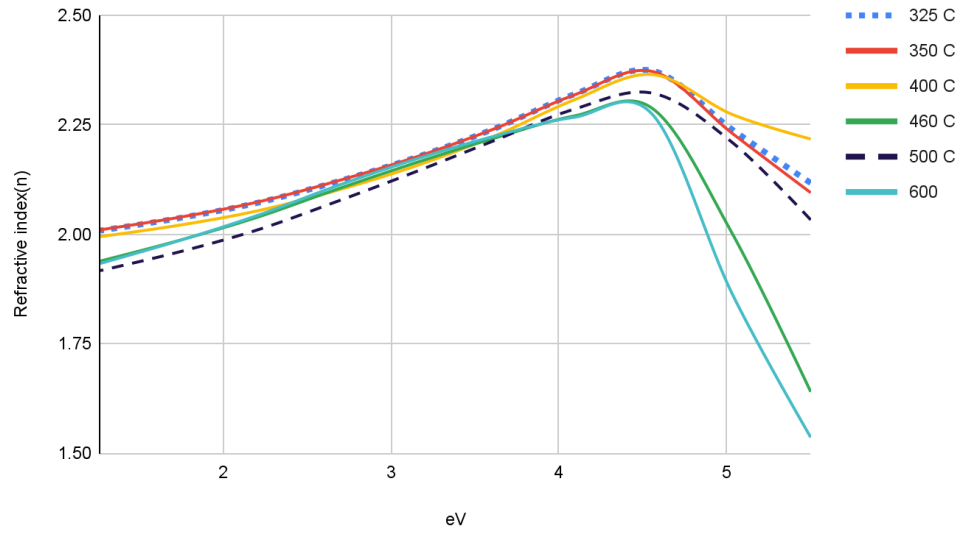


Cauchy Low Temperature

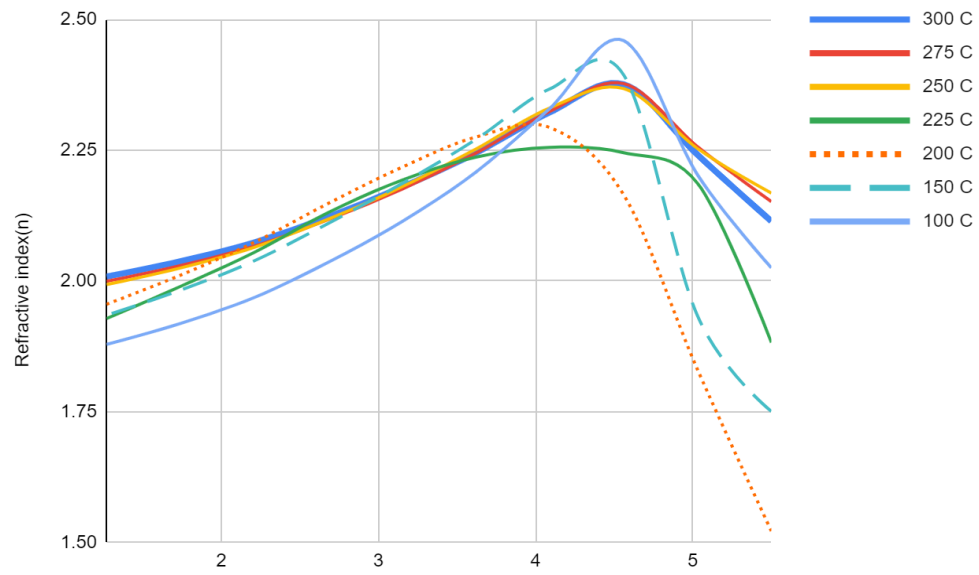


(a)

Cauchy-Lorentz

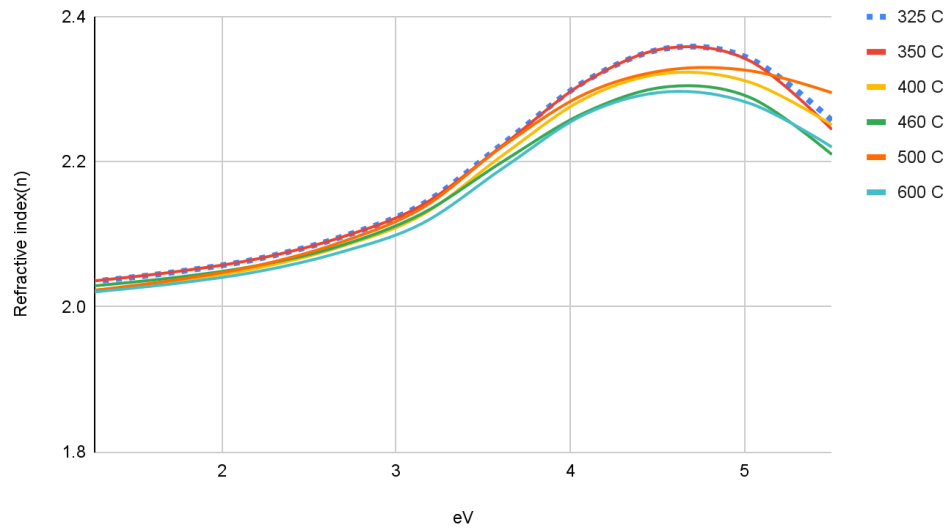


Cauchy-Lorentz (Low Temperature)

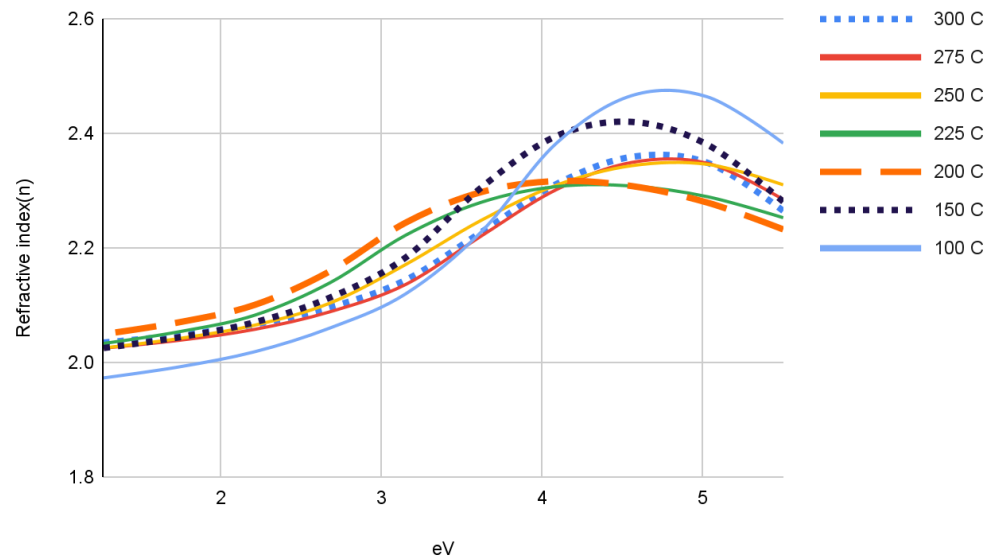


(b)

Tauc-Lorentz



Tauc-Lorentz (low Temperatures)



(c)

Fig 4: plot of refractive index against energy from various laws (a) Cauchy (b) Cauchy-Lorentz (c) Tauc- Lorentz

Cauchy Law

According to the Cauchy model in fig 4a, the majority of the films studied exhibited behavior that *deviated from logical expectations* across various energy ranges. This deviation was particularly pronounced as the films approached the ultraviolet region. These observations were consistent at both low and high temperatures. As a consequence,

it is evident that Cauchy's law is insufficient in adequately characterizing the optical properties of these films.

Cauchy-Lorentz Law

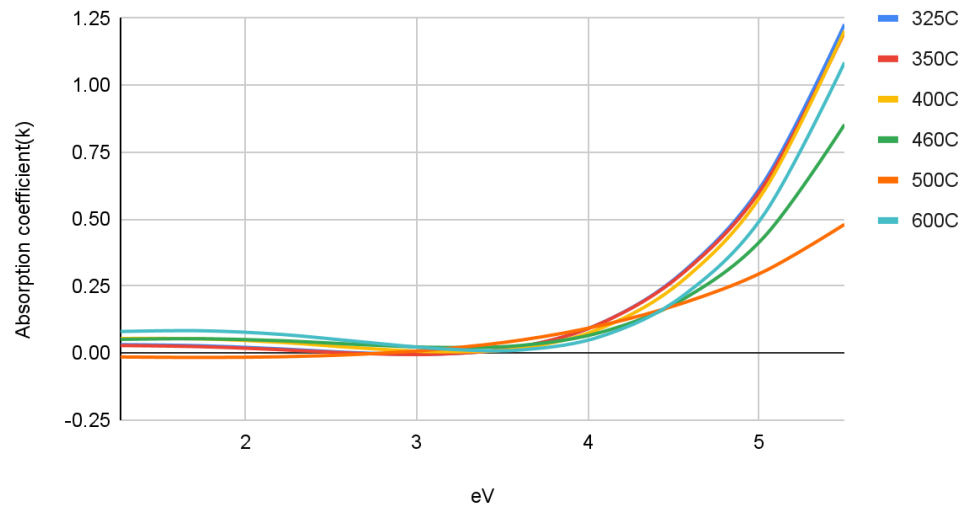
In fig 4b, this alternative representation provides improved accuracy when compared to Cauchy's law; however, prominent irregularities remain apparent as we approach the ultraviolet region. notably , a higher level of randomness is observed at low temperatures, whereas convergence of film characteristics becomes more apparent at elevated temperatures.

Tauc-Lorentz Law.

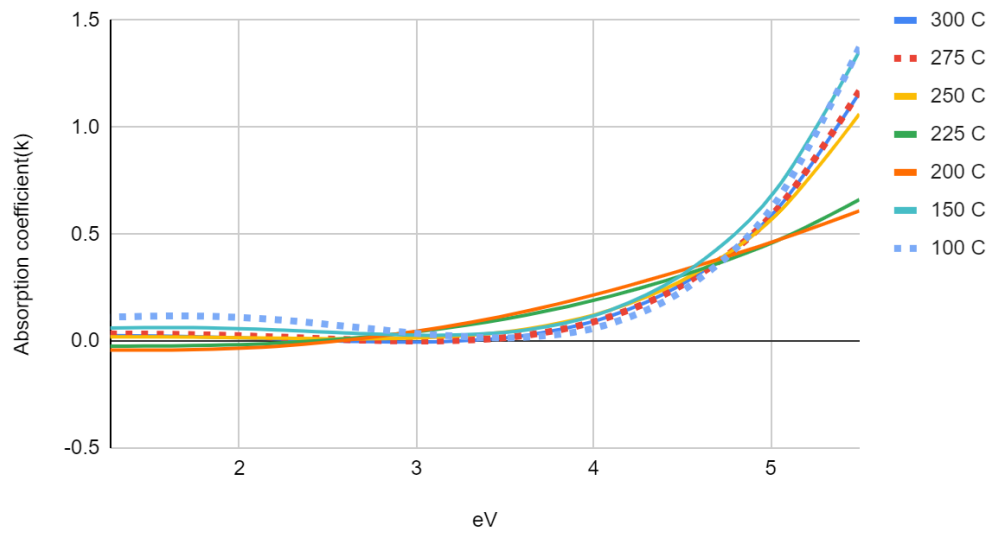
With the implementation of this law (fig 4c), the films exhibit improved logical behavior consistently across all temperatures. While some randomness persists at lower temperatures, as observed in the Cauchy-Lorentz representation, overall, there is greater uniformity and coherence in the characterisation of the films' optical properties.

4.1.2 Absorption(K) vs Energy(eV)

Cauchy (High Temp)

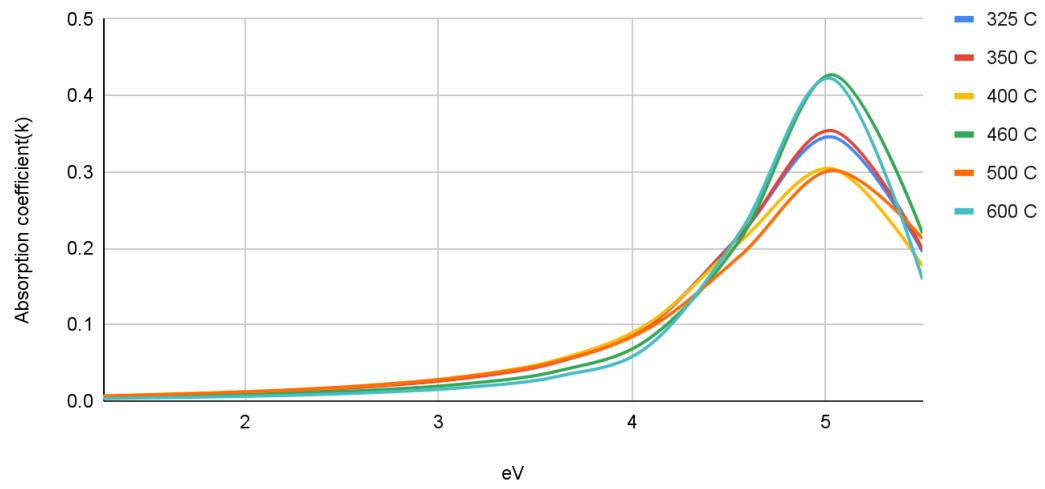


Cauchy (Low Temp)

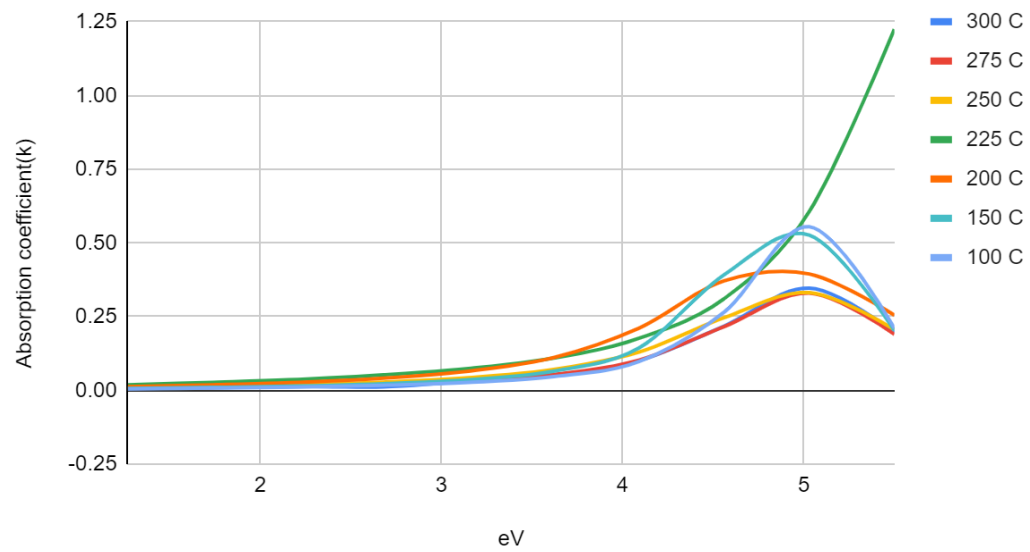


(a)

Cauchy-Lorentz (High Temp)

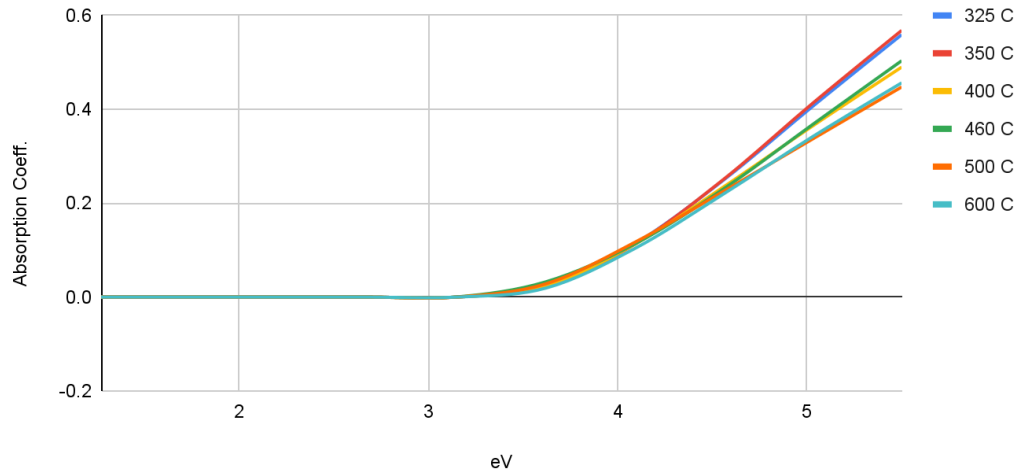


Cauchy-Lorentz (Low Temp)

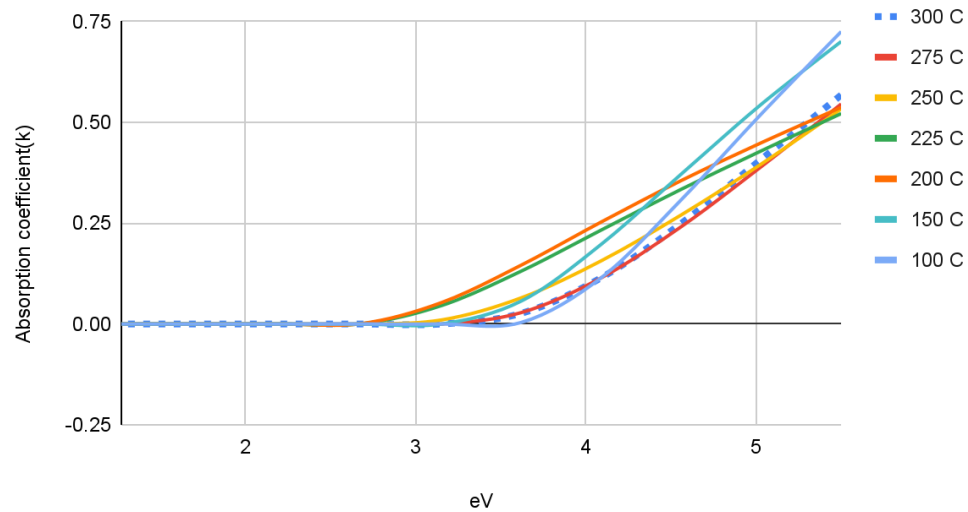


(b)

Tauc-Lorentz (High Temp)



Tauc-Lorentz (Low Temp)



(c)

Fig 4.1: plot of absorption coefficient against energy from various laws (a) Cauchy (b) Cauchy-Lorentz (c) Tauc-Lorentz

Cauchy Law

A negative absorption observed in the visible region from fig 4.1a is considered non-physical and deviates from realistic expectations. This anomaly might arise due to errors in the utilized parameters during the research. However, after careful analysis, we can confidently rule out parameter-related causes as the source of this phenomenon. In conclusion, the current law proves unsuitable for adequately describing the properties of these films, promoting the recommendation of alternative models such as Drude model, for more accurate and appropriate characterisation.

Cauchy-Lorentz

The obtained results demonstrate a more coherent outcome, except for the film at 225°C, which exhibits a significant deviation. In light of this disparity fig 4.1b, we recommend employing an alternative law to ascertain the underlying cause of the anomalous behavior. Notably in the ultraviolet region, a distinctive peak followed by a rapid reduction in absorption is observed, distinguishing it from the Cauchy model. We can not ascertain if this is bad or expected as it could represent the exciton level of these films. Further investigation is warranted to elucidate the unique characteristics exhibited in this specific region.

Tauc-Lorentz

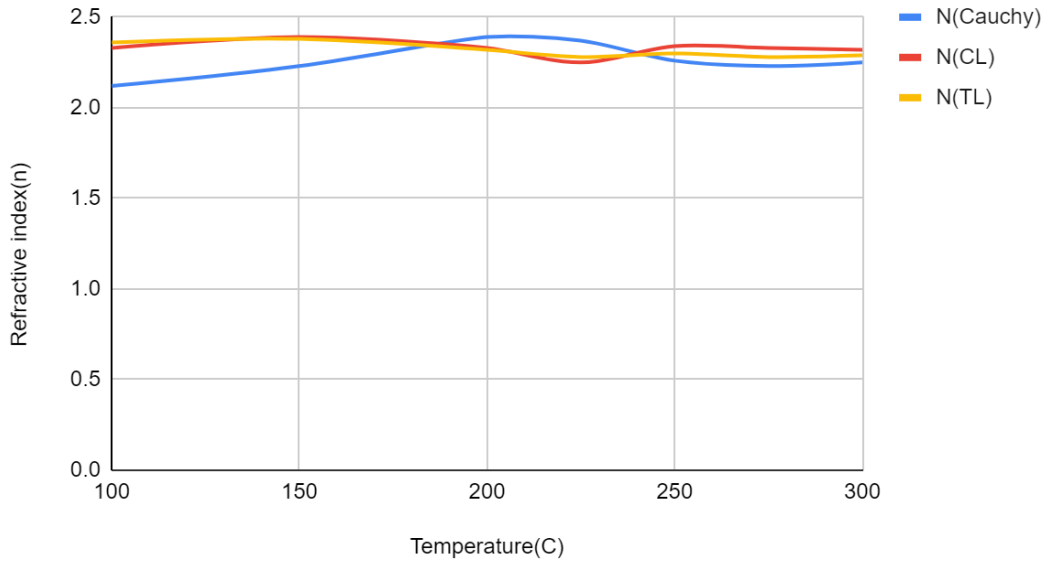
In this analysis fig 4.1c, a consistent behavior is observed among all thin films across the range of studied temperatures. A similarity with Cauchy's law is evident; however, the absence of negative absorption renders the results more realistic. Notably, as temperature increases, a more organized arrangement of film characteristics is apparent, indicating improved consistency and reliability.

4.2 Temperature(°C) Dependence:

In some applications, the temperature dependence of optical properties is of primary importance. For example, in certain scientific and engineering fields such as fiber optic sensors, precision optics in space etc, understanding how the refractive index, absorption, and other optical parameters change with temperature is critical. Temperature variations can affect the performance of optical devices and systems, particularly in environments with significant temperature fluctuations. Understanding and accounting for temperature effects are essential to ensure stability and accuracy in optical measurements and applications.

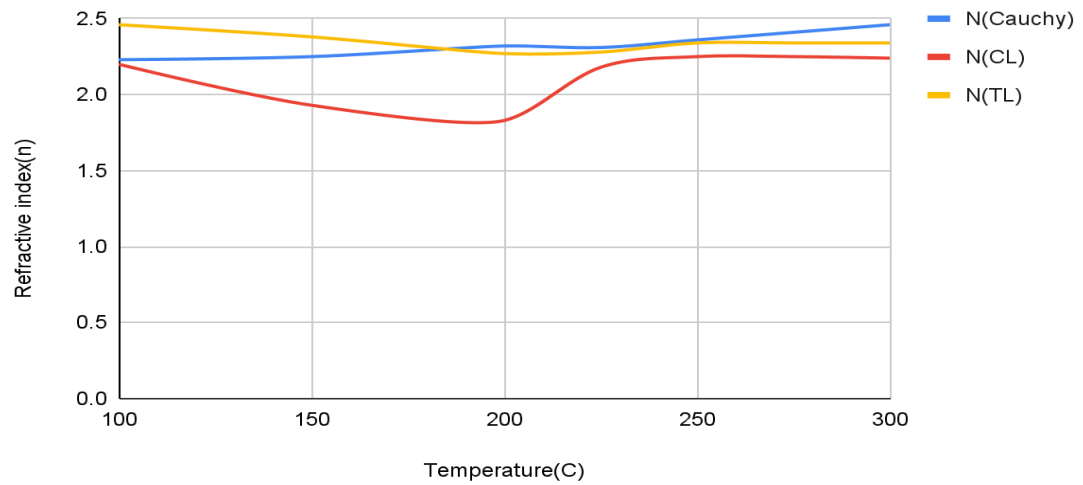
4.2.1. Refractive index(N) vs Temperature($^{\circ}$ C)

Refractive index Low temperature at 4eV



(a)

Low Temperatures at 5eV



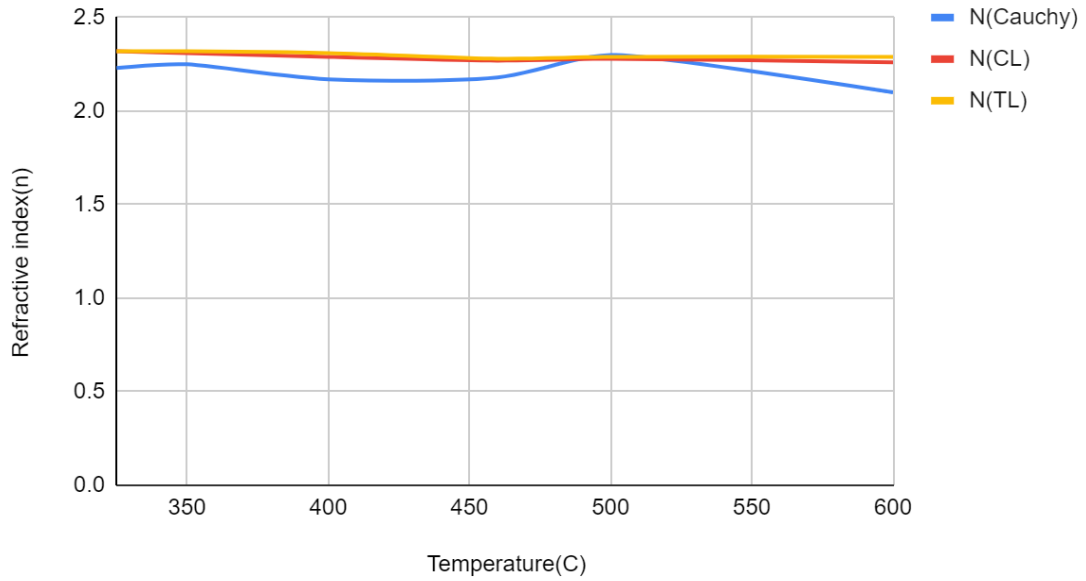
(b)

Fig 4.3 diagram showing graphs of n vs $^{\circ}$ C at (a) 4eV and (b) 5eV for low temperatures

At low temperatures, the Cauchy and TL models exhibit relatively same values for refractive index at both 4eV and 5eV. However, a notable variation is observed in the CL model at 5eV, where a decrease in the refractive index is evident until 200 $^{\circ}$ C, after which it closely resembles the behavior of the other two models utilized at both energy levels. In

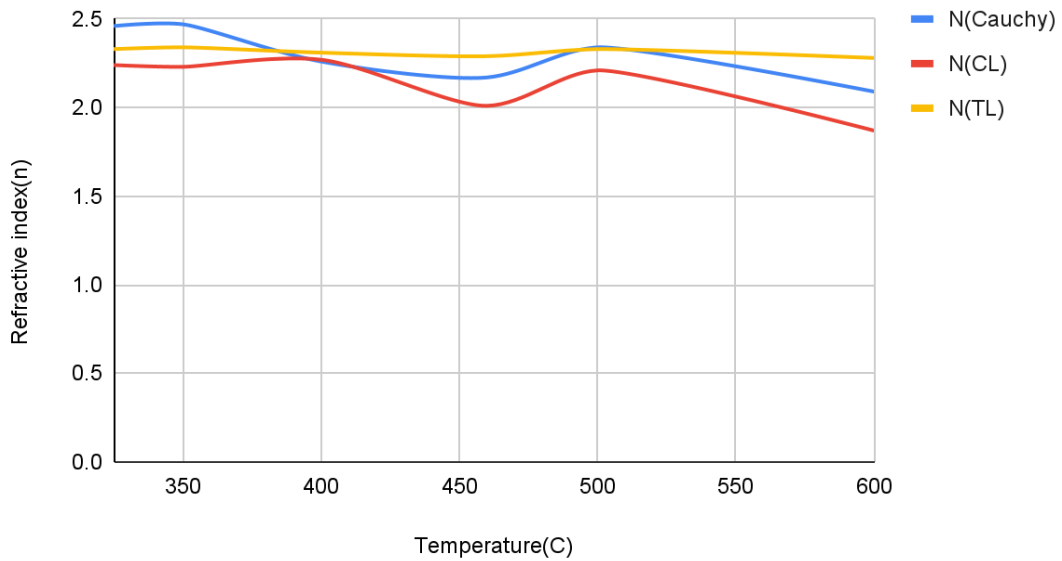
this instance, we should expect the same results across the films but since this is not so, we believe it is a problem with modeling.

Refractive index High temperature at 4eV



(a)

High Temperatures at 5eV



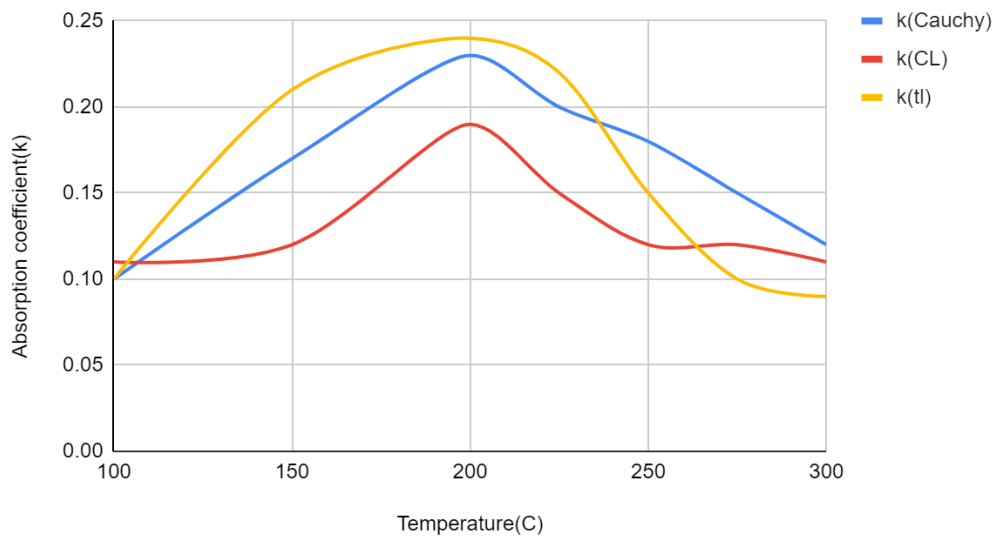
(b)

Fig 4.1: Diagram showing graphs of n vs °C at (a) 4eV and (b) 5eV for high temperature

At the energy of 5 eV, the refractive index obtained from all models falls within the range of 2.0 to 2.5, except for the CL model. The CL model exhibits multiple peaks, followed by a descending trend, ultimately reaching a value less than 2 within the temperature range of 575 °C. We can also see a modeling problem here but TL and CL showed better results.

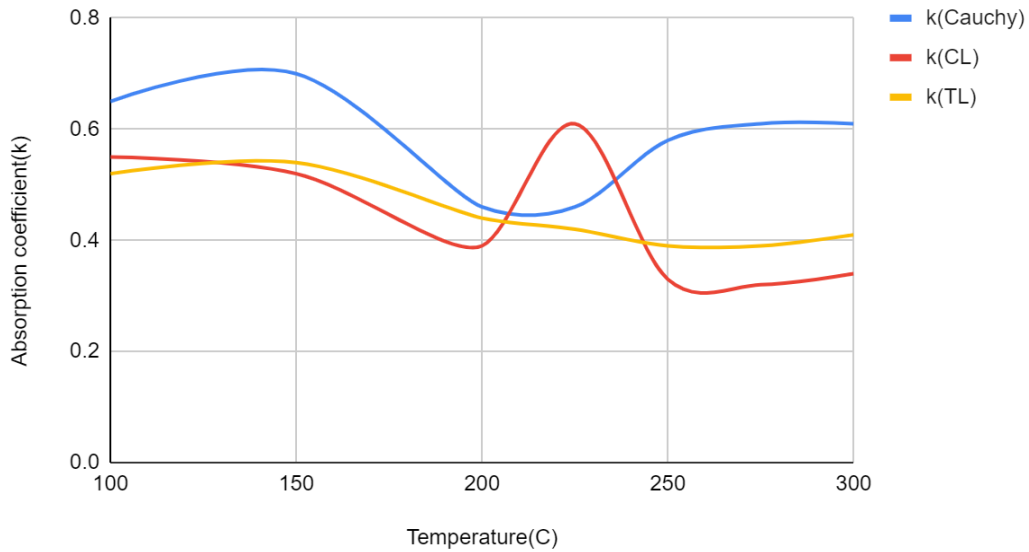
4.2.2. Absorption Coefficient(K) vs Temperature(°C)

Absorption Low temperature at 4eV



(a)

Low temperatures at 5eV



(b)

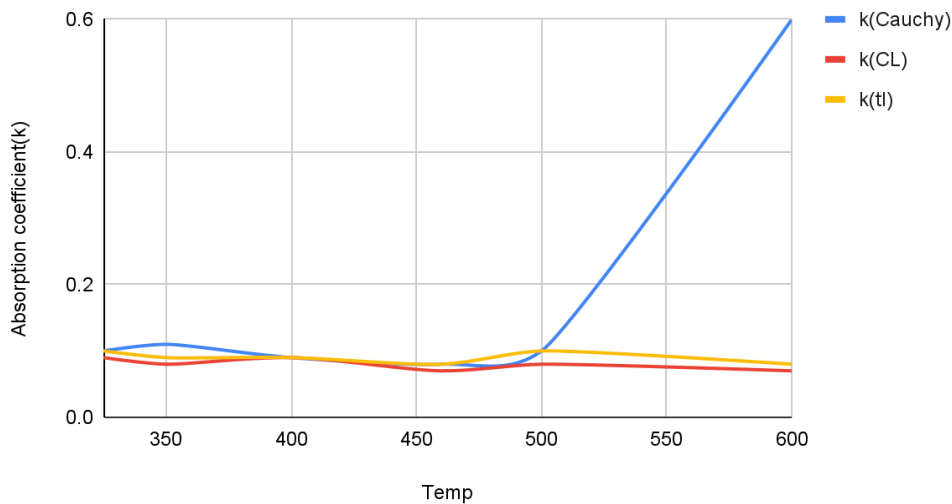
Fig 4.2 Diagram showing graphs of k vs $^{\circ}\text{C}$ at (a) 4eV and (b) 5eV for low temperature

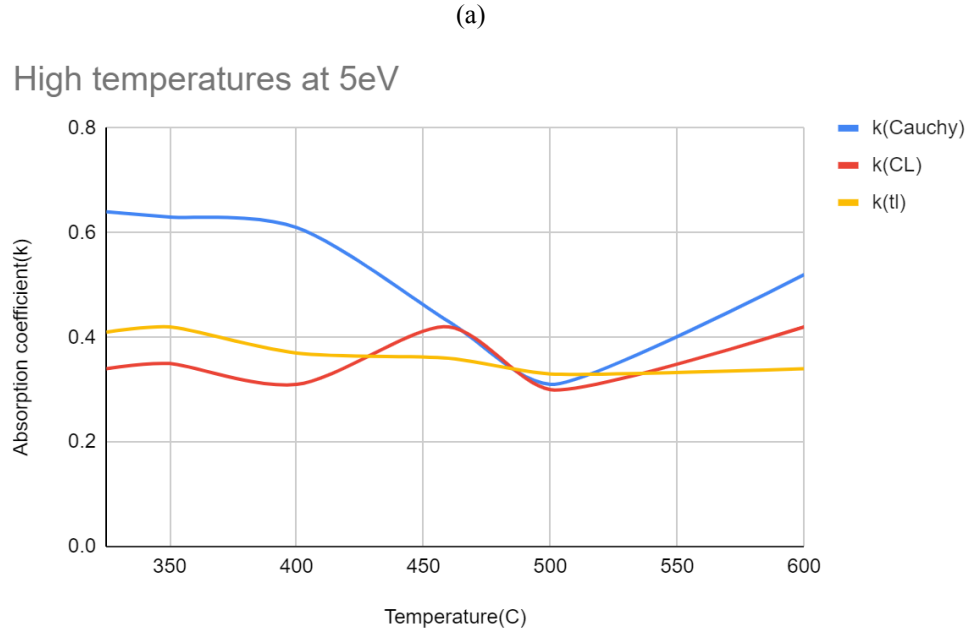
At low temperatures, specifically at 4 eV, the logical explanation is that absorption gradually increased as temperature increased, reached a peak and gradually decreased.

We assume there is some scattering at 200 $^{\circ}\text{C}$.

At the energy of 5 eV, the absorption coefficient started at a higher level for all films compared to 4 eV. Both Cauchy and CL models demonstrated more prominent peaks and descents, whereas the TL model displayed more consistent and logical responses. In summary, a gradual increase or constant absorption was observed until between 150 - 250 $^{\circ}\text{C}$, during which the films behaved randomly. There is actually no consistent way of behavior at 5 eV.

Absorption High temperature at 4eV





(b)

Fig 3: Diagram showing graphs of k vs $^{\circ}\text{C}$ at (a) 4eV and (b) 5eV for low temperature

At elevated temperatures corresponding to 4 eV, a consistent absorption behavior is observed across all temperatures for the CL and TL models. The absorption coefficient (k) maintains an approximate value of 0.1. However, a dissimilar trend is exhibited by the Cauchy model, which initially aligns with the TL and CL models until 500 $^{\circ}\text{C}$. Subsequently, there is an abrupt increase in k values, reaching approximately 0.6 for CL.

At the 5 eV, both the CL and TL models indicated an approximate constant absorption. Despite their approximate equivalence, the CL model exhibits more conspicuous peaks and descents. Conversely, the Cauchy model experiences a constant absorption but starts initially higher. Although absorption increases as temperature increases, some unpredictability could occur at 150 - 250 $^{\circ}\text{C}$ and around 500 $^{\circ}\text{C}$. Around these temperatures we could experience more or less transmission of energy as a result of excitation or presence of impurities. In general, we can not see a clearly defined behavior at this energy level.

4.3. Conclusion.

As energy increased, all the laws showed a higher refractive index. But we experienced some changes around 4 and 5 eV. At the lower temperatures there were more differences in results but as temperature increases, we noticed the films behaving more alike with respect to refractive index. After the bandgap of approximately 3.6 eV, absorption increased as energy increased. Although there are some variations with the CL model, we suggest the use of other methods such as the Drude model to observe this.

With respect to temperature dependence, the refractive index did not change very much at the ultraviolet region for both low and high temperatures. Although it would have been

more realistic if all the models were exactly alike, Cauchy showed a bit more variation, but we consider this to be a computational error.
With this research, we will be comfortable with the results provided from the TL model and suggest the films deposited at higher temperatures are of better quality.

Reference

- [1] G. Faraji, H. S. Kim, and H. T. Kashi, "Introduction," in *Severe Plastic Deformation*, Elsevier, 2018, pp. 1–17. doi: 10.1016/B978-0-12-813518-1.00020-5.
- [2] Md. M. Bellah, S. M. Christensen, and S. M. Iqbal, "Nanostructures for Medical Diagnostics," *J. Nanomater.*, vol. 2012, pp. 1–21, 2012, doi: 10.1155/2012/486301.
- [3] E. Alvaro and A. Yanguas-Gil, "Characterizing the field of Atomic Layer Deposition: Authors, topics, and collaborations," *PLOS ONE*, vol. 13, no. 1, p. e0189137, Jan. 2018, doi: 10.1371/journal.pone.0189137.
- [4] B. Macco and W. M. M. (Erwin) Kessels, "Atomic layer deposition of conductive and semiconductive oxides," *Appl. Phys. Rev.*, vol. 9, no. 4, p. 041313, Dec. 2022, doi: 10.1063/5.0116732.
- [5] A. Chowdhuri, P. Sharma, V. Gupta, K. Sreenivas, and K. V. Rao, "H₂S gas sensing mechanism of SnO₂ films with ultrathin CuO dotted islands," *J. Appl. Phys.*, vol. 92, no. 4, pp. 2172–2180, Aug. 2002, doi: 10.1063/1.1490154.
- [6] Z. Zhu, J. Ma, L. Kong, C. Luan, and Q. Yu, "Heteroepitaxy of SnO₂ thin films on m-plane sapphire by MOCVD," *J. Cryst. Growth*, vol. 324, no. 1, pp. 98–102, Jun. 2011, doi: 10.1016/j.jcrysgro.2011.04.024.
- [7] J. Sundqvist, A. Tarre, A. Rosental, and A. Hårsta, "Atomic Layer Deposition of Epitaxial and Polycrystalline SnO₂ Films from the SnI₄/O₂ Precursor Combination," *Chem. Vap. Depos.*, vol. 9, no. 1, pp. 21–25, Jan. 2003, doi: 10.1002/cvde.200290002.
- [8] M. Alaf, D. Gultekin, and H. Akbulut, "Production of Sn/SnO₂/MWCNT Composites by Plasma Oxidation After Thermal Evaporation from Pure Sn Targets Onto Buckypapers," *J. Nanosci. Nanotechnol.*, vol. 12, no. 12, pp. 9058–9066, Dec. 2012, doi: 10.1166/jnn.2012.6753.
- [9] A. Alhuthali, M. M. El-Nahass, A. A. Atta, M. M. Abd El-Raheem, K. M. Elsabawy, and A. M. Hassanien, "Study of topological morphology and optical properties of SnO₂ thin films deposited by RF sputtering technique," *J. Lumin.*, vol. 158, pp. 165–171, Feb. 2015, doi: 10.1016/j.jlumin.2014.09.044.
- [10] E. Elamurugu and K. Ramamurthi, "Optoelectronic properties of spray deposited SnO₂:F thin films for window materials in solar cells," *J. Optoelectron. Adv. Mater.*, vol. 5, Mar. 2003.
- [11] V. S. Anitha, S. Sujatha Lekshmy, and K. Joy, "Effect of Mn doping on the structural, magnetic, optical and electrical properties of ZrO₂-SnO₂ thin films prepared by sol-gel method," *J. Alloys Compd.*, vol. 675, pp. 331–340, Aug. 2016, doi: 10.1016/j.jallcom.2016.03.045.
- [12] M. Di *et al.*, "Comparison of methods to determine bandgaps of ultrathin HfO₂ films using spectroscopic ellipsometry," *J. Vac. Sci. Technol. Vac. Surf. Films*, vol. 29, no. 4, p. 041001, Jul. 2011, doi: 10.1116/1.3597838.
- [13] N. Abdullah, N. M. Ismail, and D. M. Nuruzzaman, "Preparation of tin oxide (SnO₂) thin films using thermal oxidation," *IOP Conf. Ser. Mater. Sci. Eng.*, vol. 319, p. 012022, Mar. 2018, doi: 10.1088/1757-899X/319/1/012022.